

Research Article

Characterization of NGF, $\text{trkA}^{\text{NGFR}}$, and p75^{NTR} in Retina of Mice Lacking Reelin Glycoprotein

Bijorn Omar Balzamino,¹ Filippo Biamonte,² Graziana Esposito,¹ Ramona Marino,³ Francesca Fanelli,³ Flavio Keller,³ and Alessandra Micera^{1,4}

¹ IRCCS-G.B. Bietti Foundation, Rome, Italy

² Institute of Histology and Embryology, School of Medicine "A. Gemelli", Catholic University of the Sacred Heart, Rome, Italy

³ Laboratory of Developmental Neuroscience and Neural Plasticity, University Campus Bio-Medico, Rome, Italy

⁴ Laboratory of Ophthalmology, IRCCS-G.B. Bietti Foundation, Via Alvaro del Portillo 21, 00128 Rome, Italy

Correspondence should be addressed to Alessandra Micera; amicera@gmail.com

Received 11 October 2013; Accepted 4 November 2013; Published 30 January 2014

Academic Editor: Alessio D'Alessio

Copyright © 2014 Bijorn Omar Balzamino et al. This is an open access article distributed under the Creative Commons Attribution License, which permits unrestricted use, distribution, and reproduction in any medium, provided the original work is properly cited.

Both Reelin and Nerve Growth Factor (NGF) exert crucial roles in retinal development. Retinogenesis is severely impaired in *E-reeler* mice, a model of Reelin deficiency showing specific Green Fluorescent Protein expression in Rod Bipolar Cells (RBCs). Since no data are available on Reelin and NGF cross-talk, NGF and $\text{trkA}^{\text{NGFR}}/\text{p75}^{\text{NTR}}$ expression was investigated in retinas from *E-reeler* versus control mice, by confocal microscopy, Western blotting, and real time PCR analysis. A scattered increase of NGF protein was observed in the Ganglion Cell Layer and more pronounced in the Inner Nuclear Layer (INL). A selective increase of p75^{NTR} was detected in most of RBCs and in other cell subtypes of INL. On the contrary, a slight trend towards a decrease was detected for $\text{trkA}^{\text{NGFR}}$, albeit not significant. Confocal data were validated by Western blot and real time PCR. Finally, the decreased $\text{trkA}^{\text{NGFR}}/\text{p75}^{\text{NTR}}$ ratio, representative of p75^{NTR} increase, significantly correlated with *E-reeler* versus E-control. These data indicate that NGF- $\text{trkA}^{\text{NGFR}}/\text{p75}^{\text{NTR}}$ is affected in *E-reeler* retina and that p75^{NTR} might represent the main NGF receptor involved in the process. This first NGF- $\text{trkA}^{\text{NGFR}}/\text{p75}^{\text{NTR}}$ characterization suggests that *E-reeler* might be suitable for exploring Reelin-NGF cross-talk, representing an additional information source in those pathologies characterized by retinal degeneration.

1. Introduction

Reelin and Nerve Growth Factor (NGF) take part in retinogenesis, and their increased levels occur in inflamed/degenerating retina [1–3]. Reelin is a highly conserved extracellular glycoprotein, released by neurons/accessory cells and signals via specific surface receptors belonging to the Apolipoprotein E and the very low density lipoprotein families (ApoER2 and VLDLR) and via adaptor protein Dab1 [4, 5]. Reelin expression peaks during retinogenesis, allowing migration/positioning and differentiation of retinal cells (physiological upregulation), returns to baseline levels in adulthood (physiological downregulation), and increases again following local injury/degeneration (pathological upregulation) [6, 7]. Reelin deprivation causes a macroscopic modification of the retinal structure, with incorrect cells distribution and

synaptic circuitry alteration, including a decrease in Rod Bipolar Cells (RBCs) density and an abnormal distribution of their processes in the Inner Nuclear Layer (INL), as well described in the *reeler* model [1, 8].

In the visual system, NGF exerts pleiotropic effects during development and guarantees homeostasis during adulthood [2, 3, 9–11]. NGF appears to exert multiple effects in both the neurons and accessory cells (proliferation, migration, differentiation, cytoskeletal reorganization, survival, apoptosis, etc.) [2, 3, 11]. NGF plays a crucial role during retinogenesis, influencing neuritic outgrowth, survival, and apoptosis, together with other neurotrophins and their related receptors, while in adulthood NGF is involved in several pathophysiological processes (homeostasis, ischemia, glaucoma, etc.) [2, 3, 10, 11]. NGF is produced and used in an autocrine/paracrine fashion by Retinal Ganglion Cells (RGCs), Bipolar and other

retinal cell types (horizontal and amacrine cells, Müller glia) [11]. The biological effects of NGF are directly dependent on the specific binding to two different cell surface receptors, the tyrosine kinase $\text{trkA}^{\text{NGFR}}$ and the glycoprotein p75^{NTR} [12, 13]. NGF/ $\text{trkA}^{\text{NGFR}}$ promotes the survival and recovery of RGCs, as observed in experimental models and after intraocular injection of NGF [2, 11, 14, 15]. The crucial contribution of the $\text{trkA}^{\text{NGFR}}/\text{p75}^{\text{NTR}}$ ratio in the survival of RGCs has been recently envisaged [13, 15]. Previous studies showed an impaired NGF expression in Reelin-deficient mice [16, 17].

In view of all these findings a possible cross-talk between NGF and Reelin during retinal development might be hypothesized, suggesting an abnormal NGF pathway in Reelin-deficient retinas. To address this question, a homozygous *reeler* mice model was developed from founder couples and used to investigate both the biochemical and molecular expression of NGF- $\text{trkA}^{\text{NGFR}}/\text{p75}^{\text{NTR}}$.

2. Materials and Methods

2.1. Ethics Statement. All experiments were performed in compliance with the ARVO Statement for the Use of Animals in Ophthalmic and Vision Research. Animal care procedures were conducted in conformity with the Intramural Committee and Institutional guidelines, in accordance with national and international laws and policies (EEC Council Directive 86/609, OJ L 358, 1, December 12, 1987; NIH Guide for the Care and Use of Laboratory Animals, NIH Publication 85-23, 1985). The experimental protocol was approved by the Ethical Committee of “Tor Vergata” University (Rome, Italy).

2.2. Animals and Genotyping. Founder couples of *reeler* strain (B6C3Fe-a/a-rl; Jackson Laboratories, Bar Harbor, ME, USA), carrying the $\text{rl}^{\text{lx-/-}}$ mutation in a C57BL/6J background, were purchased from Charles River (Calco, Italy). The colony was housed at animal house facility (“Tor Vergata” University) under standard conditions (12 hrs light/dark cycle, temperature $21 \pm 1^\circ\text{C}$, and relative humidity $60 \pm 10\%$). Both water and food were freely available (Enriched Standard Diet, Mucedola, Settimo Milanese, Italy). To obtain the double-mutant *reeler*-L7-EGFP strain (referred to as *E-reeler* in this study), B6C3Fe-a/a-rl and B6-FVB-Tg (Pcp2-EGFP)2Yuza/J strains (Jackson Laboratories) were crossed and then backcrossed, according to a standard procedure [18]. The offspring from the 8th generation were used as donors that were hemizygotes for the Green Fluorescent Protein (GFP) locus. The B6C3Fe-L7-EGFP mice were used as control (wild-type $\text{rl}^{\text{lx+/+}}$ genotype; E-control). Since GFP expression is under control of the L7 promoter, high levels of this live cell marker (lacking toxicity) characterize RBCs and allow their easy analysis at confocal microscopy (resistant to bleaching) [19].

For the present study, a total of $n = 62$ eyes (31 mice) were used and grouped as follows: $n = 32$ *E-reeler* eyes (21 ± 1 days; body-weight range: 9–11 g) and $n = 30$ E-control eyes (21 ± 1 days; body-weight range: 12–14 g). In a pilot study, RBCs were quantified at P7, P14, P21, and P35, in order to choose the best

time-point for analyses ($n = 3$ /time-point; $n = 9$ *E-reeler*, and $n = 3$ E-control).

EGFP expression and *reeler* genotype were assessed as previously reported, with minor modifications [20, 21]. Briefly, 1 μg DNA was extracted from tails and placed in a 10x reaction buffer (100 mM Tris-HCl, pH 8.3, 500 mM KCl, and 15 mM MgCl_2) containing 10 mM dNTPs, 20 μM random primers, and 5 U/mL recombinant Taq polymerase (Euroclone, Milan, Italy). DNA amplification was performed in a PTC-100 cyclor (MJ Research Inc., Watertown, MA). Specific primers for GFP detection and genotyping studies were synthesized by Invitrogen (Grand Island, USA). Detailed primer sequences, gene accession number and amplification profiles are reported in Table 1(A). DNA products and ladder (100 bps molecular marker; Takara Bio Inc., Shiga, Japan) were separated in 0.8–1.5% agarose gel containing ethidium bromide (0.5 $\mu\text{g}/\text{mL}$; Appligene Oncor). Gels were acquired by the Kodak EDAS 290 imaging system (Kodak, Tokyo, Japan).

2.3. Tissue Sampling. *E-reeler* and E-control mice were deeply anaesthetized by 2 mg/mL ketamine (0.2 mL/10 gr body-weight; Ketavet, Gellini Farmaceutici, Italy) and 0.23 mg/mL medetomidine (0.24 mL/10 gr body-weight; Domitor, Orion Corp., Espoo, Finland) intraperitoneal injection.

For confocal microscopy analysis, mice were perfused through the left ventricle with saline solution (3 min), followed by 4% buffered paraformaldehyde (PFA; 5 min). Enucleated eyes ($n = 10$ eyes for *E-reeler* and $n = 8$ eyes for E-control) were postfixed in the same fixative (48 hrs) and cryoprotected in 10% sucrose (24 hrs).

For molecular and biochemical analysis, mice were sacrificed by cervical dislocation and the retinas were quickly processed for biochemical ($n = 8$ eyes each, for both *E-reeler* and E-control) or molecular ($n = 14$ eyes each, for both *E-reeler* and E-control) analysis. The dissection of retinas from fresh enucleated eyes was carried out under a dissector microscope (SMZ645; Nikon, Tokyo, Japan), equipped with cold-light optic fibers (PL2000 photonic; Axon, Vienna, Austria).

2.4. Immunofluorescence and Digital Analysis. Postfixed and cryoprotected eyes were quickly frozen in dry ice, embedded in OCT medium (TissueTek; Leica, Heidelberg, Germany), and sectioned (CM3050 cryostat; Leica Microsystems, Rijswijk, The Netherlands). Serial sections (7 μm) were placed ($n = 3$ sections/slide, $n = 6$ slides/retina) onto gelatinized slides, preheated to increase tissue attachment, and stored at -20°C . Both antigen retrieval (0.05% trypsin-EDTA solution, 2 min) and blocking/permeabilizing (1% BSA and 0.5% Triton X100 in PBS, 15 min) steps were performed before the addition of specific antibodies: anti-NGF (sc-549), anti- $\text{trkA}^{\text{NGFR}}$ (sc-118), and anti- p75^{NTR} (sc-6188) antibodies, all from Santa Cruz Biotech (Santa Cruz, CA). A quenching passage was also carried out to minimize PFA background and slightly reduce the higher fluorescent expression of the E-construct. Cy3-conjugated donkey

TABLE 1: Primers for genotyping (A) and for real time PCR (B) used in the study.

^a Gene access number	Sequence (For/Rev)	Amplicon	Annealing conditions
A: genotyping			
^b Reeler (GM75)	F: 5'-TAA TCT GTC CTC ACT CTG CC-3'	380 bp	55°C, 120 s
^b Reeler (3W1)	R: 5'-ACA GTT GAC ATA CCT TAA TC-3'	280 bp	
^b Reeler (3R1)	R: 5'-TGT ATT AAT GTG CAG TGT TG-3'		
^a GFP 1	F: 5'-CGT AAA CGG CCA CAA GTT CAG-3'	500 bp	65°C, 30 s
^a GFP 2	R: 5'-ATG CCG TTC TTC TGC TTG TCG-3'		
B: RT-PCR			
^c GAPDH	S: 5'-GTGGACCTCATGGCCTACAT-3'	100 bp	53°C, 30 s
BC059110	AS: 5'-GTTGGGATAGGGACTCCTCAC-3'		
^c trkA	S: 5'-AACAAACGGCAACTACAC-3'	137 bp	58°C, 25 s
M23102	AS: 5'-CCTGTTTCTCCGTCCAC-3'		
^c p75 ^{NTR}	F: 5'-GAGGCACCACCGACAACCTC-3'	131 bp	55°C, 25 s
AF187064	R: 5'-TGCTTGCAGCTGTTCCACCT-3'		
^c NGF	F: 5'-CTGGCCACACTGAGGTGCAT-3'	120 bp	53°C, 30 s
BC011123	R: 5'-TCCTGCAGGGACATTGCTCTC-3'		

Amplification profiles:

^a 1 cycle at 94°C/5 min, 30 cycles including 94°C/1 min, 55°C/2 min, and 72°C/3 min, and a final cycle at 72°C/10 min.

^b 1 cycle at 94°C/5 min, 35 cycles including 94°C/30 sec, 65°C/30 sec, and 72°C/30 sec, and a final cycle at 72°C/10 min.

^c 1 cycle at 95°C/15 min, 47 cycles of denaturation at 95°C/30 sec, annealing at 55–60°C/25 sec (primer's T_m dependent), and elongation at 72°C/30 sec, fluorescence monitoring at 60–90°C, 0.01°C for 0.3 sec, and final incubation at 72°C/5 min. Single melting curves always verified.

species-specific antibodies (1:500–700; Jackson ImmunoResearch Europe Ltd., Suffolk, UK) were used to bind all primary antibodies. Nuclear counterstaining was performed with TOTO3-Iodide (Molecular Probes, Eugene, OR) while GFP expression specifically identified RBCs [19]. Isotypes (negative controls) were carried out in parallel with the omission of primary antibodies and used for appropriate channel series acquisition and related background subtractions. Slides were coverslipped using a glycerol gelatin mounting medium (Sigma-Aldrich, St. Louis, CA). Serial images were acquired by CI software connected to an inverted microscope (Eclipse TE2000U, Nikon). Digital images (pixel size: 512 × 512 or 1024 × 1024 dpi) were saved, converted into 8-bit TIFF images, and subjected to densitometric analysis (Image J v1.43; NIH-<http://rsb.info.nih.gov/ij/>). Single integrated optical density (IntDen) was registered for *E-reeler* and E-control retina ($n = 5$ optic fields/slide/retina; ×40/dry 0.75 DIC M/N2), in terms of specific RBCs density and dendrite length ($n = 5$ sections/animal). IntDen data were collected: mean values (±SD) were calculated and subjected to statistical analysis. Quantification of RBCs in retinas was performed by evaluating the number of the GFP-expressing RBCs in the INL. A grid of 27 × 18 fields (field size: 25 μm × 27.5 μm) was printed onto a transparent sheet and attached to the screen of a 15" LCD-display. Three representative regions were analysed as follows: left, right, and across the optic nerve over five consecutive slides/mice/experimental group. Cells outside the region of interest were automatically ignored and the results were averaged as a percentage of positive cells. All counts were performed under blind conditions and presented as mean ± SD.

2.5. *Western Blot*. Dissected retinas were homogenized in 70 μL modified RIPA Buffer (50 mM Tris-HCl, 150 mM NaCl, 1% Triton-X100, 5 mM EDTA, 100 mM NaF, and 1 mM PMSF; pH 7.5) and briefly sonicated to shrink DNA (VibraCell equipped with microtip; Sonics & Materials, Inc., Newtown, USA) [22]. Total proteins were quantified with the DC protein assay kit (BioRad Laboratories Inc., Hercules, CA), by using the A1000 Spectrophotometer (Nanodrop, Celbio, Milan, Italy). Normalized samples (50 μg) were subjected to 7.5% or 12% SDS-PAGE, under reducing conditions (130 V/frontline; Miniprotean apparatus, Biorad). Electrophoresed proteins were transferred onto Hy-Bond membranes (GE Healthcare, Buckinghamshire, UK), in the presence of 48 mM Tris-Cl (pH 6.8), 39 mM glycine, 0.0037% SDS, and 20% methanol solution (10 V/55 min; semidry condition, Transblotting apparatus, Biorad). Membranes were stained with 0.5% Ponceau S in acetic acid (ICN, Milan, Italy) to verify protein transfer, washed twice in 0.5% Triton X100-Tris buffered saline (TBS: 20 mM Tris-HCl and 150 mM NaCl, pH 7.5) for 30 min, and blocked in 0.05% Tween-20 TBS (TW-TBS) containing 5% nonfat dry milk for 1 hr. The membranes were then probed (4°C/18 hrs) with the following primary antibodies: anti-NGF (sc-549), anti-trkA^{NGFR} (sc-118), anti-p75^{NTR} (sc-6188) from Santa Cruz, and anti-Actin (ab-3280) from Abcam (Cambridge, UK). Membranes were washed in TW-TBS and subsequently incubated with POD-conjugated donkey species-specific antibodies (1:30000; Jackson ImmunoResearch) for 90 min. Detection of specific signal was performed by using an enhanced Chemi-Luminescent system (West Femto Sensitivity Substrate; Pierce, Rockford, IL). Alternatively, membranes were exposed to Hybond filters in appropriate cassette and developed in appropriate solutions. Both

membranes and filters were acquired by 1D Image Station (Kodak). Data were saved as 8-bit TIFF files and exported to be shown after Adobe Photoshop CS3 assembly (Adobe System, San Jose, CA). Densitometric analysis was performed using the 1D Image software (Kodak) and related Optical Density (OD) values, referred to as normalized samples, were shown in bar plots.

2.6. Real Time PCR Amplification. Dissected retinas were pretreated with Proteinase K (20 mg/mL, 56°C/3 hrs; Finnzyme, Milan, Italy) in modified HIRT buffer (50 mM Tris-Cl, pH 8, 1 mM EDTA, 1% Tween20). Total RNA was extracted 1:1 with TRIfast, according to a standard procedure (EuroClone), and resuspended in 10 µL fresh RNase free water (Direct Q5, Millipore Corporation, Billerica, MA). To eliminate any genomic DNA contamination, all total RNA samples were treated with RNase-free DNaseI, according to the supplier's protocol (2 U/µL; AM-1907; Turbo DNA free kit; Ambion Ltd., Huntingdon, Cambridgeshire, UK). Total RNA samples were checked for RNA quantity/purity (>1.8; A280 program, Nanodrop) and for absence of RNA degradation (1% agarose gel analysis). Equivalent amounts of RNA (1 µg) were used as template to generate cDNAs, according to the IMPROM manufacturer's procedure (Promega Corp., Madison, USA), in a one cyler programmable thermocycler (PqLab Biotech, Erlangen, Germany). The resulting cDNAs were amplified using the SYBR Green PCR core reagent kit (Applied Biosystems, Foster City, CA) in an Opticon2 programmable thermocycler (MJ Research), according to standard procedures [23]. Samples were amplified in duplicate and in parallel with negative controls (either without template or with mRNA as template). Real cycle thresholds (Cts) were recorded during linear amplification and normalized to those of referring genes run in parallel ($nCts = Ct_{target} - Ct_{referring}$). Averages were calculated from these replicates and expressed as normalized Ct or as expression ratio of a normalized target gene (fold changes in log₂-scale), according to REST[®] analysis [24]. Both primer sequence and amplification profile are accurately reported in Table 1(B). The specific primers were designed using Primer3 software (<http://www.primer3.com>) and synthesized by MWG Biotech (Ebersberg, Germany). GenBank software was used to select the complete mRNA sequence of each gene investigated (<http://www.ncbi.nlm.nih.gov/> Genbank; provided by the National Center for Biotechnology Information, Bethesda, MD). Primer specificities were confirmed by single melting curves, monitored during amplification. In random tests, PCR products were separated on 2.5% agarose gel and acquired by 1D Kodak software to verify the presence of a single amplicon.

2.7. Statistical Analysis. All data are shown as mean ± SD (in text) and mean ± SEM (in bar plots). Parametric ANOVA analysis followed by a Tukey-Kramer post hoc comparison was used to estimate differences between groups [25]. The statistical package used was StatView II for PC (Abacus Concepts Inc., Barkley, CA). REST/ANOVA coupled analysis was carried out for molecular comparisons. $trkA^{NGFR}/p75^{NTR}$

ratio was calculated according to the single Cts values recorded during linear amplification and normalized to those of referring genes run in parallel (nCts), where Cts are inversely proportional to mRNA expression [22]. Kendall's rank coefficient (Tau) was also calculated to identify correlation between GFP versus $p75^{NTR}$ and $trkA^{NGFR}$ versus $p75^{NTR}$. A probability of $P < 0.05$ was presumed to reflect statistical significant difference between groups.

3. Results

A preliminary observation of *E-reeler* mice was carried out between P7 and P35 showing ataxia, eating complications (typical of *reeler* mice), and survival difficulties for the majority of animals, in the absence of appropriate handling [1]. Accordingly, the P21 time-point was selected for the following studies of characterization, and only *E-reeler* mice carrying both the *reeler* mutation and EGFP expression were included in the study. The genotyping is shown in Figure 1(a): as depicted in (A), a 500 bp band was observed in *E-reeler* and E-control DNA extracts, as compared to a negative control, confirming the positive EGFP genotyping; as depicted in (B), two DNA fragments were observed in DNA extracts: one corresponding to the wild-type allele (280 bp; WT) and the other to the *reelin* allele (380 bp; RI). Both bands are visible in the heterozygous mouse, not used in these studies.

According to Oberdick and coworkers procedure, both *E-reeler* and E-control retinas express GFP-specific fluorescence mainly localized in the dendrites, soma, and axon terminals of RBCs, allowing their easy recognition with confocal microscopy [20]. As shown in Figure 1(b) (merge), a decrease in the number (arrows) and dendrite length of RBCs populating the INL, as well as their synaptic buttons (arrowheads) in the GCL, was observed in *E-reeler* retinas. Digital analysis carried out on serial images showed a 27.2% decrease in GFP immunoreactivity in *E-reeler* retina (20899 ± 4663 versus 28727 ± 8134 IntDen, resp., *E-reeler* versus E-control; $P < 0.001$). GFP-bearing RBCs were also counted in serial sections, showing a 27.8% decrease in the *E-reeler* retinas as compared to E-control ones (resp., 209 ± 4 versus 287 ± 81 cells/optic field; $P < 0.001$; Figure 1(c)).

3.1. NGF Expression. In order to understand whether NGF is affected in *E-reeler* retina, serial sections were probed with specific NGF antibody and NGF immunoreactivity was evaluated in the INL and GCL. As shown in Figure 2(a), NGF immunoreactivity was increased in RBCs, as well as in both GCL and other INL cells (arrowheads) of *E-reeler* retina. Therefore, the digital analysis carried out on these sections showed a 13.9% increase of NGF immunofluorescence in *E-reeler* retinas (32705 ± 2197 versus 27756 ± 1124 IntDen, resp., *E-reeler* versus E-control; $P < 0.05$). In line with this result, Western blot and the related OD measurements showed a 37.4% NGF increase (both 12 and 15 kDa bands) in the *E-reeler* ($P < 0.05$; Figure 2(b)). Finally, the molecular analysis of *E-reeler* mRNA extracts did not show a significant effect on NGF mRNA expression (0.39_{2log} ratio; 7.21 ± 1.05 versus 7.43 ± 1.89 nCts, resp., *E-reeler* versus E-control; $P > 0.05$).

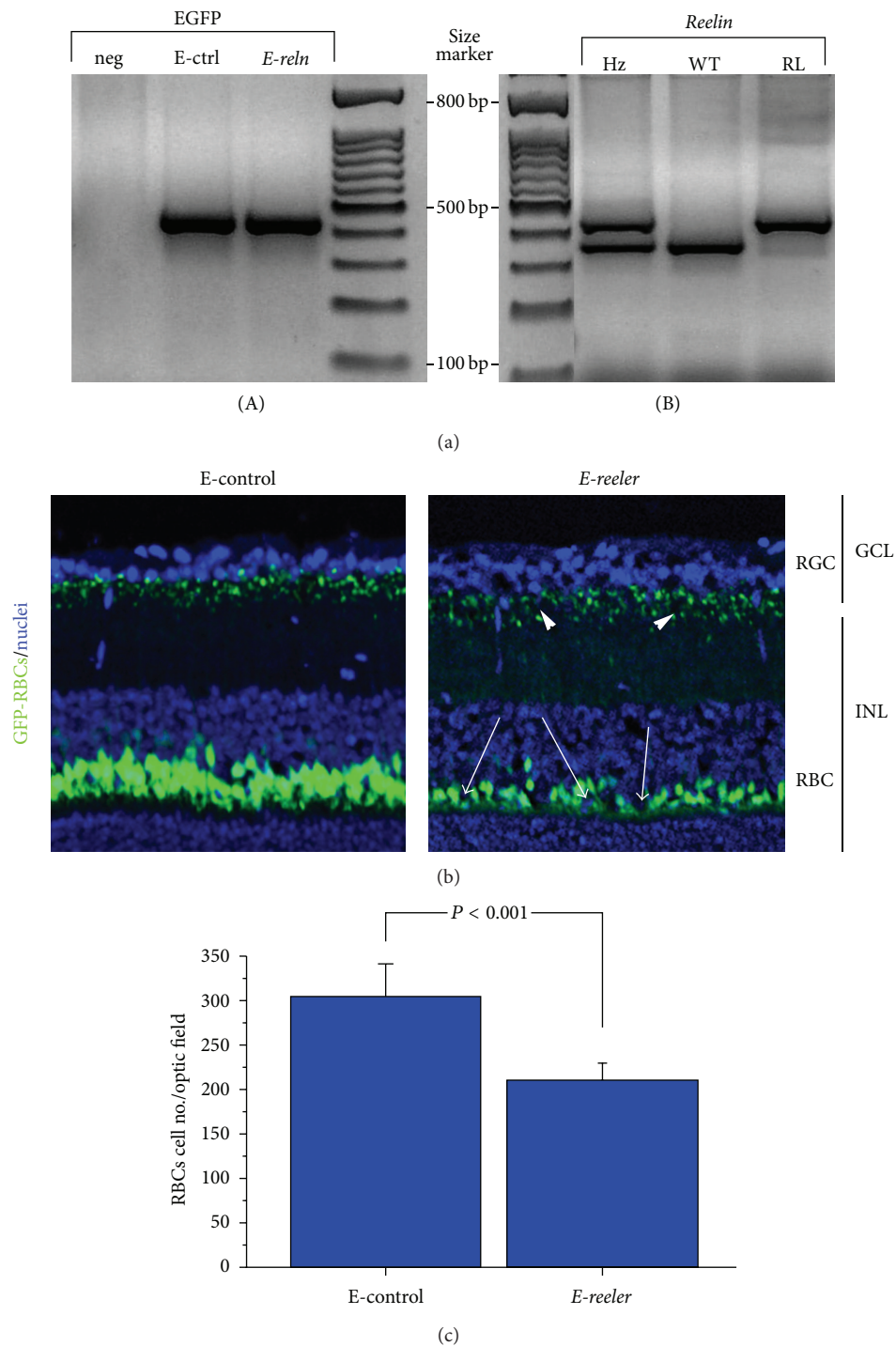


FIGURE 1: *E-reeler* model. (a) Agarose gel representative of EGFP and *Reelin* gene amplification. (A) EGFP expression in E-control (E-ctrl) and *E-reeler* (*E-reln*) tail genome, with respect to negative control (neg), not expressing GFP linked to L7-EGFP construct; (B) *Reelin* expression in control (WT), heterozygote (Hz), and *reeler* (RL). The higher band (380 bps) represents *reeler* status while the lower one (280 bps) represents control rank. (b) Representative confocal microscopy image showing GFP-expressing RBCs (green) and nuclei stained with TOTO3-Iodide (blue). A decrease in the number of RBCs populating the INL is visible in *E-reeler* retina (arrows), as compared to E-control counterpart. Note the reduction of GFP-fluorescence of both the dendrite length and synapses (GFP staining) indicated by arrowheads in the *E-reeler* retinas ($\times 400$). (c) Number of GFP-bearing RBCs in *E-reeler* retinas, compared to the E-controls. Note the significant decrease of fluorescent cells ($P < 0.001$). Abbreviations: GFP, Green Fluorescent Protein; RGCs, Retinal Ganglion Cells; INL, Inner Nuclear Layer; RBCs, Rod Bipolar Cells.

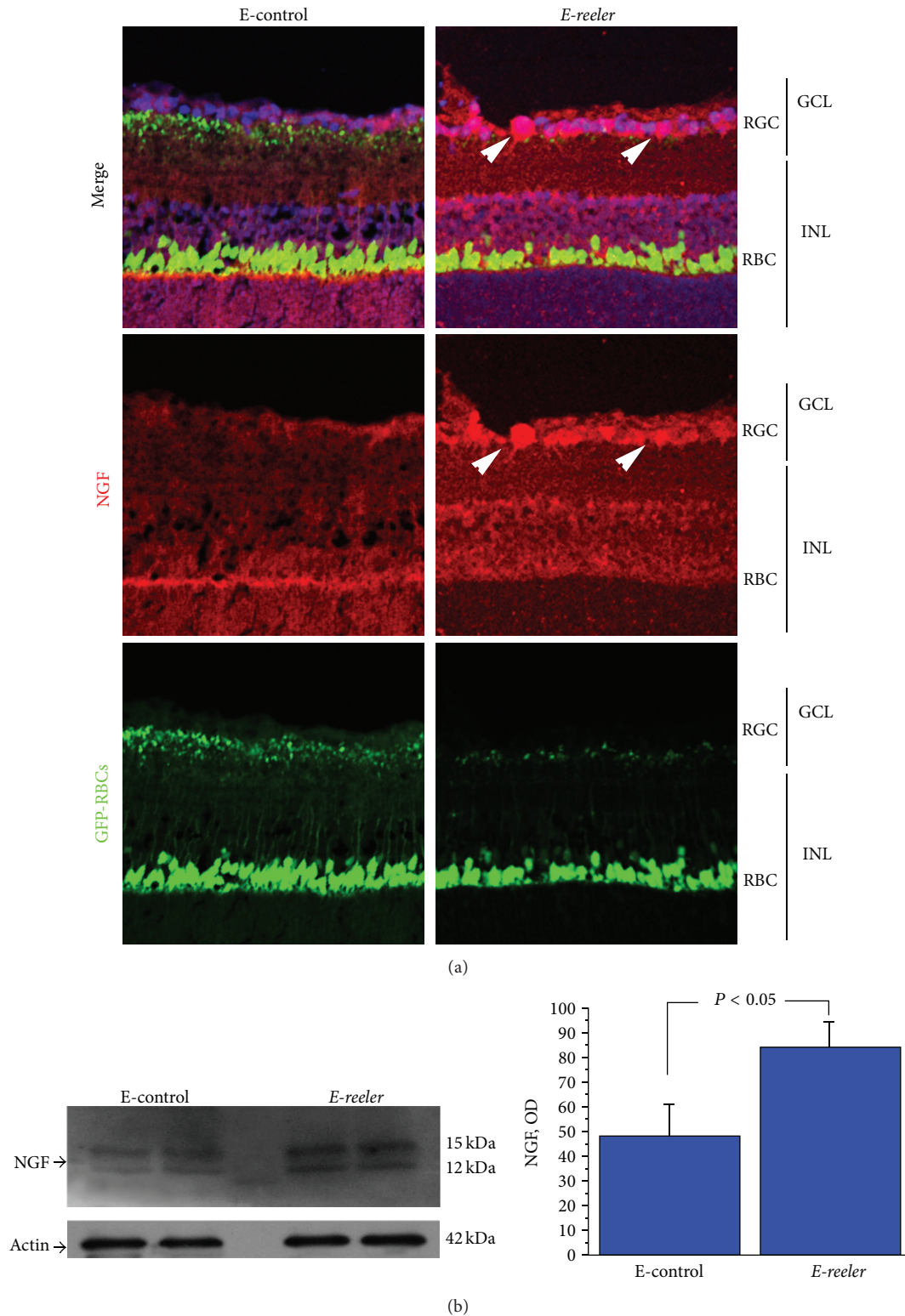


FIGURE 2: Expression of NGF in *E-reeler* retina. (a) Confocal microscopy showing images of GFP-expressing RBCs (green), NGF immunoreactivity (red), and nuclear staining (blue). As indicated by arrowheads, in the merge and NGF single staining, INL cells strongly immunoreacted with the NGF antibody. Some immunoreactivity was also observed in other structural and accessory cells ($\times 400$). (b) Representative 12% SDS-PAGE and relative densitometric analysis of E-control and *E-reeler* retinal extracts probed with the NGF antibody (OD values; $P < 0.05$). The size-marker was run between the two groups. Abbreviations: GCL, Ganglion Cell Layer; INL, Inner Nuclear Layer; RGCs, Retinal Ganglion Cells; RBCs, Rod Bipolar Cells; GFP, Green Fluorescent Protein; OD, Optical Density.

3.2. *trkA*^{NGFR} Expression. Since *trkA*^{NGFR} is widely considered the main NGF receptor involved in cell migration, proliferation, and differentiation, *trkA*^{NGFR} protein expression was investigated by probing both *E-reeler* and E-control retinas. As shown in Figure 3(a), *trkA*^{NGFR} immunoreactivity was detected in both the INL and GCL of control retinas (merge). A trend towards a 5.64% decrease of *trkA*^{NGFR} immunoreactivity was quantified in the RGCs of *E-reeler* retinas (22601 ± 2391 versus 23953 ± 1278 IntDen, resp., *E-reeler* versus E-control; $P > 0.05$). Accordingly, Western blot and OD analysis did not show any significant *trkA*^{NGFR} differences between the *E-reeler* versus the E-control protein extracts (Figure 3(b)). These results were corroborated by molecular analysis ($-0.14_{2\log}$ ratio; 17.04 ± 1.81 versus 16.63 ± 0.54 nCts, resp., *E-reeler* versus E-control; $P > 0.05$).

3.3. *p75*^{NTR} Expression. Given that NGF binds to *p75*^{NTR}, the expression and localization of this glycoprotein were also investigated. In *E-reeler* retinas, *p75*^{NTR} immunoreactivity increased in RBCs, RGCs, and other INL populating cells, as highlighted by arrows in (Figure 4). Densitometric analysis quantified a 44.7% increase of *p75*^{NTR} immunoreactivity in the *E-reeler* retina (19587 ± 1916 versus 13539 ± 1368 IntDen, resp., *E-reeler* versus E-control; $P < 0.05$). In line, Western blot analysis coupled to densitometric quantification showed a significant 32.5% increase of *p75*^{NTR} in *E-reeler* protein extracts ($P < 0.05$; Figure 5(a)). The increased *p75*^{NTR} protein expression in *E-reeler* retinas was corroborated by real time PCR ($1.69_{2\log}$ ratio; 4.29 ± 1.77 versus 5.73 ± 3.22 nCts; *E-reeler* versus E-control; $P < 0.05$). The decrease of RBCs (GFP⁺ cells) did not correlate significantly with the increase of *p75*^{NTR} immunoreactivity (OD), as detected by Kendall rank analysis between the *E-reeler* and E-control values (Tau = -0.308 ; $P > 0.05$). Interestingly, the *trkA*^{NGFR}/*p75*^{NTR} ratio (from nCts values) was decreased in *E-reeler* mice as compared to the E-controls, indicating a shift towards *p75*^{NTR} expression (Tau = 0.867 ; $P < 0.01$, Figure 5(b)).

4. Discussion

This study was undertaken to verify the NGF-*trkA*^{NGFR}/*p75*^{NTR} expression in retinas from *E-reeler* mice, a Reelin-deprived model showing severe structural and functional changes in the retina, alongside the severe central nervous system alterations. To date, no data are available on the NGF pathway in Reelin deficient retina.

Retinogenesis is driven by a milieu of soluble factors, synergizing to obtain the final well-organized synaptic circuitry [1, 8]. As observed in several experimental models, Reelin and NGF take part actively during retinogenesis and continue all over adulthood, contributing to retina homeostasis (synaptic plasticity) [1, 3, 7, 8]. Structural and functional changes in the retina have been detected in Reelin deficient mice, showing an altered distribution of RBCs (both cell malpositioning and reduced dendrite density) and impaired synaptic circuitry [1]. RGC apoptosis has been quantified upon chemical NGF deprivation, while the recovery of damaged structures and

particularly NGF/*trkA*^{NGFR}-promoted RGC survival were observed upon the intraocular NGF injection, as observed in models of retinal degeneration (ischemia, glaucoma, and diabetes) [11, 26–28].

Since emerging data lead to a possible cross-talk between Reelin and NGF during retinogenesis and tissue remodeling, the well-characterized *reeler*-L7-EGFP model was developed (*E-reeler*) and Reelin-deprived retinas underwent NGF-*trkA*^{NGFR}/*p75*^{NTR} confocal microscopy and biomolecular characterization [16, 17]. The morphological analysis of *E-reeler* retina at P7-P35 showed structural changes characterized by altered arrangement and significant decrease of axon/dendrite density of residual RBCs (retina degeneration), in line with previous studies [1, 6, 8]. Ataxia and eating and survival difficulties were observed, and since the survival was highly reduced over P27 in the absence of appropriate management, the P21 was definitely selected for these studies. According to the digital analysis and the conventional cell-counting method, significant reductions in RBCs' soma, dendrites, and axons were quantified in *E-reeler* retina. This observation is in line with previous studies indicating that just RBCs represent the primary target of Reelin defect, even though both RBCs and RGCs express/react to Reelin [1, 5]. Since RBCs carry the signal from the rod photoreceptors to the RGCs (visual function), it is reasonable to hypothesize that RBCs defect might interfere with the physiological activity of RGCs in *E-reeler* retina.

The principal finding of this study is the significant increase of NGF all over *E-reeler* retina, mainly localized in the layers populated by RBCs (INL) and RGCs (GCL). Indeed, NGF immunoreactivity was greatly expressed in accessory/glia cells, representing certainly the main NGF source in the damaged neighbourhood [29–32]. The observation of increased NGF protein, not corroborated by the molecular data, might be explained as possible transcriptional/posttranscriptional regulations (differential regulation, stability, and degradation of mRNA). In line with the well-known NGF pleiotropic effects, this NGF increase might be explained as an endogenous compensatory response to Reelin deficiency, either to limit abnormal/impaired cell distribution or counteract undesired apoptosis [12, 26, 33].

The statement that NGF exerts multiple effects depending on the surface (co)receptor appearance strength suggests the potential contribution of *trkA*^{NGFR} and/or *p75*^{NTR} in this model. In the retina, *p75*^{NTR} privileges Müller glial cells while *trkA*^{NGFR} is mainly expressed by RGCs [30, 34]. While *trkA*^{NGFR} tasks in neuronal survival, growth, and synaptic modulation are well established, *p75*^{NTR} ones are still an open debate due to *p75*^{NTR}-*trkA*^{NGFR} coreceptor activity/complexity [15, 33, 35]. *p75*^{NTR} mediates a widespread range of cellular functions, depending on the cell-to-cell and/or cell-to-factor milieu as well as the repertoire of surface (co)receptors and can signal independently of *trkA*^{NGFR} [12, 36, 37]. In the nervous system, *p75*^{NTR} mediates neuronal survival by facilitating *trkA*^{NGFR} signal, increasing neuronal axon growth and reducing neuronal cell death [37–42]. As a second finding, a significant increase of *p75*^{NTR} and a trend towards

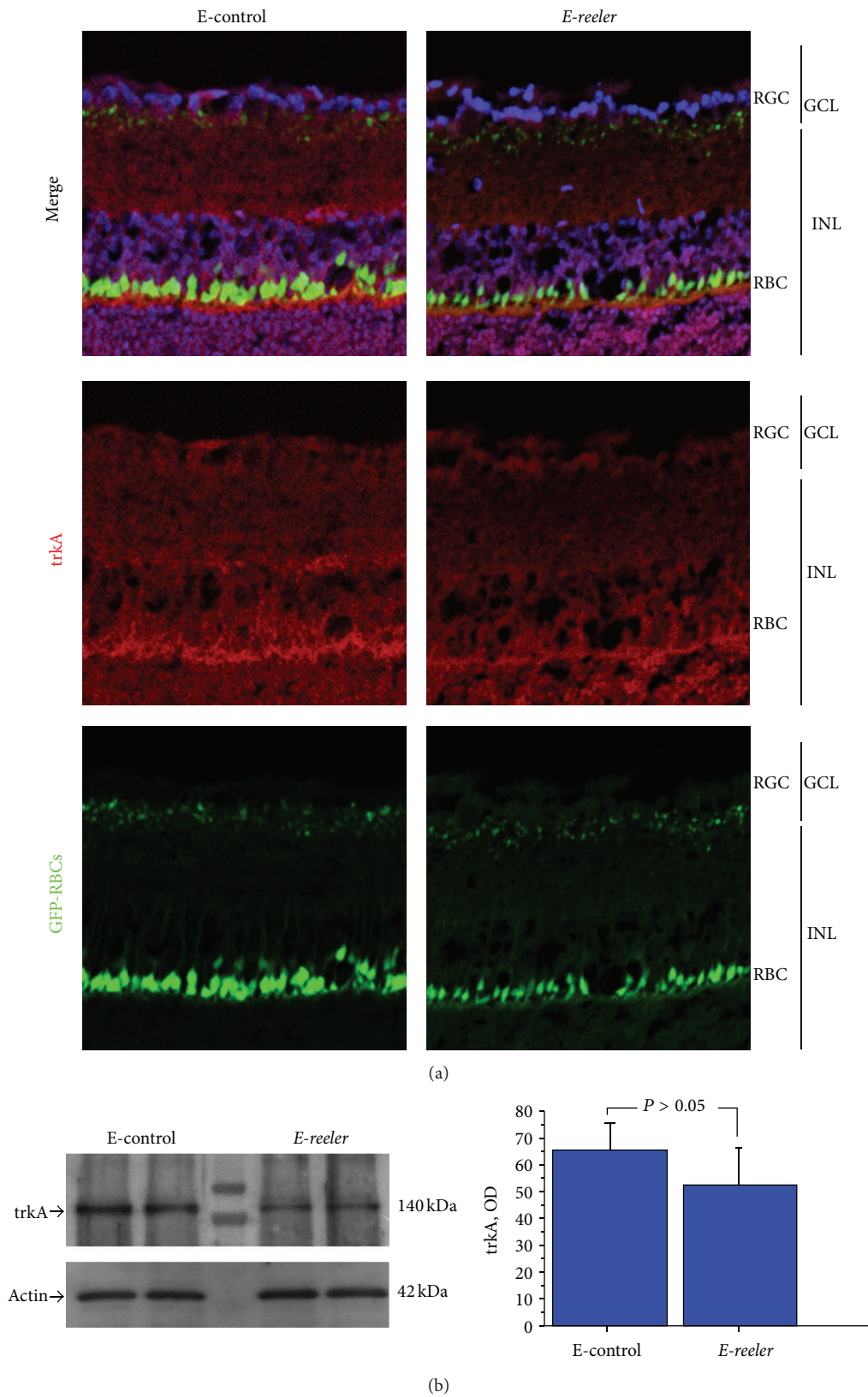


FIGURE 3: Expression of $trkA^{NGFR}$ in *E-reeler* retina. (a) Confocal microscopy showing images of GFP-expressing RBCs (green), $trkA^{NGFR}$ immunoreactivity (red), and nuclear staining (blue). A weak $trkA^{NGFR}$ immunoreactivity was observed at the RBCs (body and dendrites). $trkA^{NGFR}$ staining was less intense across the INL and in some cells inside the GCL of the *E-reeler* retina ($\times 400$). (b) Representative 7.5% SDS-PAGE and relative densitometric analysis of E-control and *E-reeler* retinal extracts probed with the $trkA^{NGFR}$ antibody (OD values; $P > 0.05$). The size-marker was run between the two groups. Abbreviations: GFP, Green Fluorescent Protein; RGC, Retinal Ganglion Cells; GCL, Ganglion Cell Layer; INL, Inner Nuclear Layer; RBCs, Rod Bipolar Cells; OD, Optical Density.

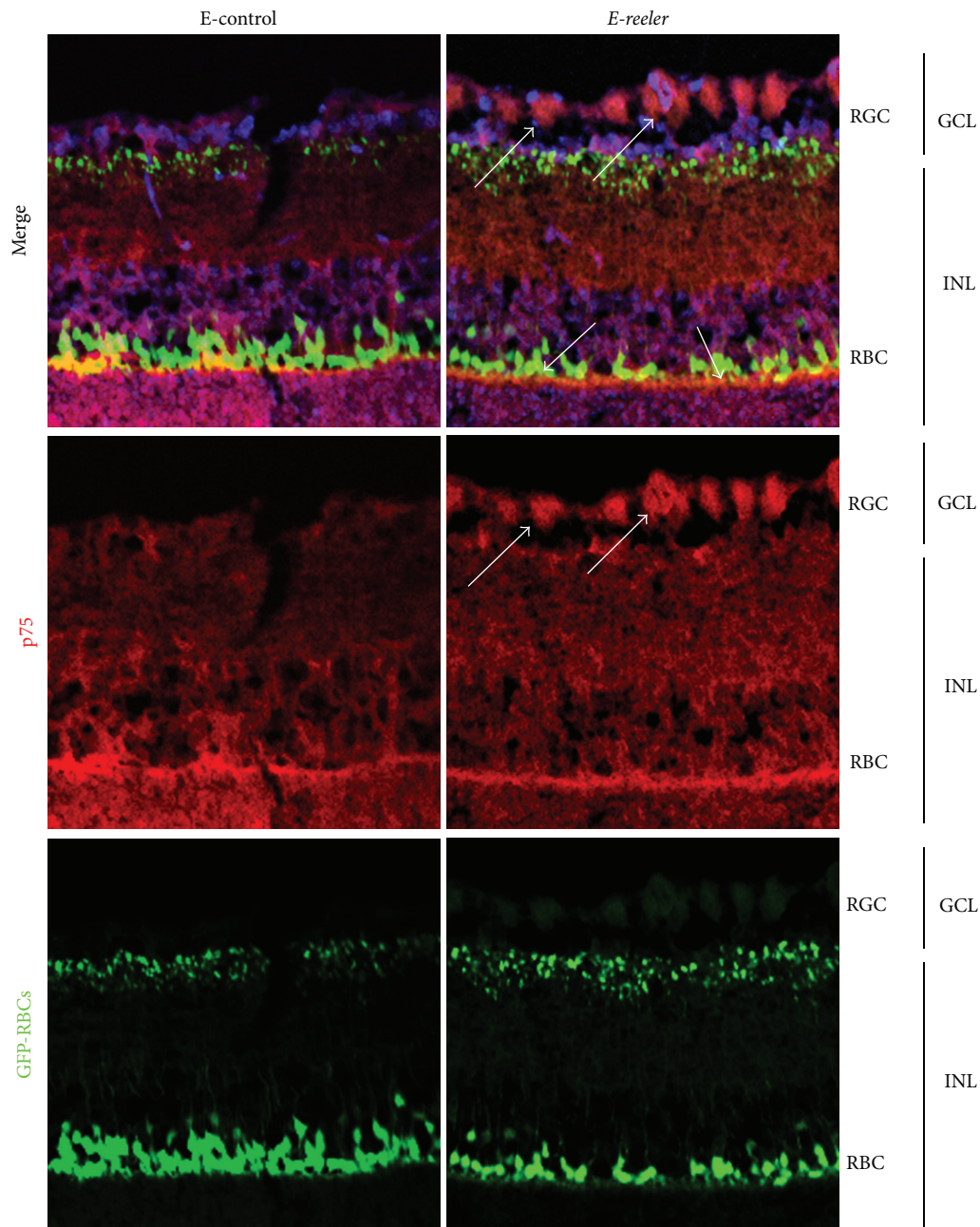


FIGURE 4: $p75^{\text{NTR}}$ localization in *E-reeler* retina. Confocal microscopy showing images of GFP-expressing RBCs (green), $p75^{\text{NTR}}$ immunoreactivity (red), and nuclear staining (blue). Arrows point to a noticeable staining of RGCs, RBCs, and accessories/glia cells localized in the GCL/INL of *E-reeler* retina. Note the intense cytoplasmic $p75^{\text{NTR}}$ localization in both RGCs and RBCs. Abbreviations: GFP, Green Fluorescent Protein; GCL, Ganglion Cell Layer; INL, Inner Nuclear Layer; RGCs, Retinal Ganglion Cells; RBCs, Rod Bipolar Cells ($\times 400$).

a decrease of $\text{trkA}^{\text{NGFR}}$ were observed in *E-reeler* retina, as detected by confocal microscopy, Western blot, and real time PCR analysis. Interestingly, $p75^{\text{NTR}}$ was mainly localised in RBCs and cells populating the GCL, either RGCs or accessory ones. In particular for GCL, whether $p75^{\text{NTR}}$ is expressed by immature/migrating or mature/positioned RGCs during retinogenesis (or in adult retina) remains to be verified, as accessory cells processed tightly surround RGCs [28, 42, 43]. This $p75^{\text{NTR}}$ expression would imply

that NGF from RGCs and nearby accessory cells might promote the survival of interneurons (and likewise RBCs) via NGF/ $p75^{\text{NTR}}$ -dependent mechanism, favouring a “rescue response” in an autocrine/paracrine fashion [11, 27, 28, 39]. The contribution of $p75^{\text{NTR}}$ in the regulation of RBCs survival has been reported in an experiment of exposure to NGF, BDNF, or Neurotrophin 3 [44]. Therefore, the possibility that $p75^{\text{NTR}}$ might exert the herein reported actions through other growth factors cannot be excluded [12, 27].

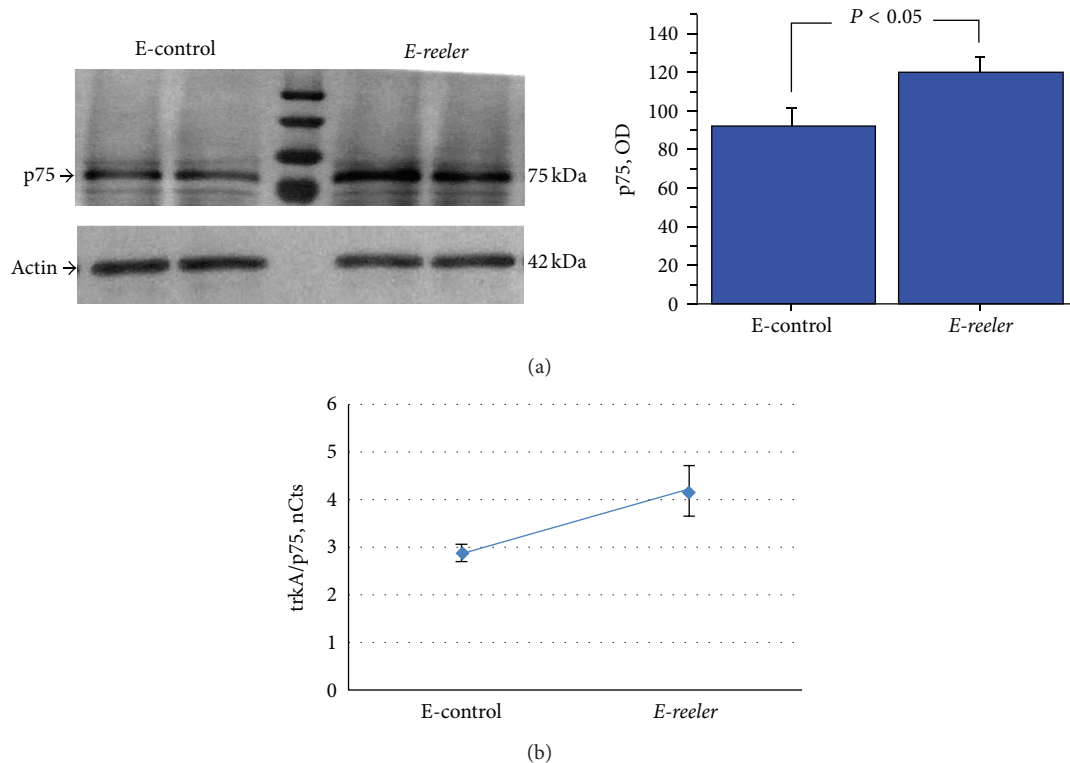


FIGURE 5: p75^{NTR} expression in *E-reeler* retina. (a) Representative 7.5% SDS-PAGE and relative densitometric analysis (OD values; $P < 0.05$), probed with p75^{NTR} antibodies, showing a significant increase of p75^{NTR} in *E-reeler* protein extracts, as compared to the E-control. (b) Scatter plot showing the correlation with the $\text{trkA}^{\text{NGFR}}/\text{p75}^{\text{NTR}}$ ratio in the *E-reeler* versus E-control, highlighting a shift towards p75^{NTR} expression (Tau = 0.857; $P < 0.01$).

An attempt for cytoskeleton reorganization might be also prospected for NGF and p75^{NTR} overexpression, since p75^{NTR} is strictly required for appropriate axonal morphology/outgrowth and cell migration [38]. Actin reorganization and cell migration as well as neurite outgrowth are common properties of both NGF and Reelin [1, 4–7, 26, 27]. As reported, the loss of RGCs might be an outcome of the reduced crosstalk with the RBCs (synapses decline) [1]. NGF overexpression in RGCs or accessory/Müller cells might be also viewed as an attempt to stimulate RBC dendrites/arbor elongation, to (re)establish synaptic connections, or to provide a gradient for new dendrites [45–48]. As a support, p75^{NTR} binds both pro/mature forms of NGF and other neurotrophins (NTs, BDNF, NT3, and NT5), takes part in retrograde axonal transport of NTs (as survival or apoptotic factor), and works as a shuttle molecule for BDNF and NT4 (RBC survival NTs) [44, 49]. As reported, NGF pathway contributes to the cytoskeleton reorganization, at least in structural cells as myofibroblasts [50].

By the way, the selective shift toward p75^{NTR} expression does not exclude the potential contribution of $\text{trkA}^{\text{NGFR}}$ signalling. As reported, p75^{NTR} acts as neuroprotective molecule, and $\text{trkA}^{\text{NGFR}}$ might work as a death receptor [43, 51]. Upon NGF exposure, both homo- and heterodimerizations of membrane bound $\text{trkA}^{\text{NGFR}}$ and p75^{NTR} occur on receptive cells, and the ultimate signalling response is the result of

some predominant cascade pathways [12, 13]. The dogma “ $\text{trkA}^{\text{NGFR}}$ mediates survival while p75^{NTR} triggers apoptosis” is strictly dependent on the cell type, microenvironment, and $\text{trkA}^{\text{NGFR}}/\text{p75}^{\text{NTR}}$ surface-expression ratio [12, 15]. In line with our finding, a possible role of $\text{trkA}^{\text{NGFR}}/\text{p75}^{\text{NTR}}$ ratio in determining the fate of RBCs and RGCs might be prospected, as supported by studies on degeneration rescue [11, 14, 15]. Therefore the p75^{NTR} increase in RGCs and RBCs might also be interpreted as a proapoptotic effect. Studies aimed at verifying/quantifying apoptosis of RGC and/or RBC are actually under investigation.

As widely reported, a milieu of soluble factors synergize to allow for the correct position and functional activity of the RGCs, amacrine cells, RBCs, horizontal cells, Müller glial cells, and rod/cone photoreceptors during retinogenesis [8, 52]. The possibility that upon Reelin deprivation other factors (cytokines and growth and angiogenic factors) might be upregulated to offset or facilitate the entire process cannot be excluded. Beside NGF, several other factors (such as BDNF, NT4, and GDNF) have been reported to increase RGC survival and regeneration [44, 53]. These activities might be direct or indirect as observed for NGF-p75^{NTR}-induced TNF- α and TGF- β activities in developing retina [54].

Any attempt to comprehend the mechanism underlying the pathogenesis of some retinal disorders represents a step forward in ophthalmology field characterized by

severe, invalidating, and life-threatening diseases (glaucoma, ischemia, retinopathies, etc.). One of the major challenges of current eye-disease research is to develop models that mimic eyes pathologies, useful tools for studying cell-to-cell and cell-to-mediator mechanisms and providing the basis for novel therapeutic approaches to offset retinal degeneration. Despite recent advances, a clear comprehension of the mechanism underlying retinopathies is still needed and might require the understanding of some “missing” aspects during retinogenesis. For several decades, the *reeler* mutant has been used as a model for studying neurological disorders [1, 16]. In line with recent and the herein presented data, we propose *E-reeler* mice as a good “retinal disease” model to explore the cross-talk between NGF and Reelin [16, 17]. Growing data indicate that NGF provides a potential approach in the treatment of retinopathies, characterized by RGCs death and following optic nerve degeneration [2, 3, 10, 11]. Studies are underway to discriminate p75^{NTR}-induced cell rescue or apoptosis and characterize the proNGF/NGF expression. These studies will contribute to better understanding of the relationship between NGF and Reelin in the retina under normal and pathological conditions.

Conflict of Interests

The authors declare that there is no conflict of interests regarding the publication of this paper.

Acknowledgments

This work was partially supported by the Italian Minister of Health to IRCCS-Biotti and the Italian Ministry of Education to UCBM (PRIN 2009P9CE2R). The authors are grateful to Professor Marco Centofanti, Glaucoma Research Unit (“Tor Vergata” University, Rome, Italy), for suggestions during the preparation of the paper. The study was partially presented at the annual meeting of the Association for Research in Vision and Ophthalmology, Fort Lauderdale, FL, May 2012 (E-Abstract).

References

- [1] D. S. Rice, S. Nusinowitz, A. M. Azimi, A. Martínez, E. Soriano, and T. Curran, “The Reelin pathway modulates the structure and of retinal synaptic circuitry,” *Neuron*, vol. 31, no. 6, pp. 929–941, 2001.
- [2] G. Carmignoto, M. C. Comelli, P. Candeo et al., “Expression of NGF receptor and NGF receptor mRNA in the developing and adult rat retina,” *Experimental Neurology*, vol. 111, no. 3, pp. 302–311, 1991.
- [3] N. Berardi and L. Maffei, “From visual experience to visual function: roles of neurotrophins,” *Journal of Neurobiology*, vol. 41, no. 1, pp. 119–126, 1999.
- [4] E. Förster, H. H. Bock, J. Herz, X. Chai, M. Frotscher, and S. Zhao, “Emerging topics in Reelin function,” *European Journal of Neuroscience*, vol. 31, no. 9, pp. 1511–1518, 2010.
- [5] J. H. Trotter, M. Klein, U. K. Jinwal et al., “ApoER2 function in the establishment and maintenance of retinal synaptic connectivity,” *Journal of Neuroscience*, vol. 31, no. 40, pp. 14413–14423, 2011.
- [6] G. D’Arcangelo, “The role of the Reelin pathway in cortical development,” *Symposia of the Society for Experimental Biology*, no. 53, pp. 59–73, 2001.
- [7] J. S. Pulido, I. Sugaya, J. Comstock, and K. Sugaya, “Reelin expression is upregulated following ocular tissue injury,” *Graefes Archive for Clinical and Experimental Ophthalmology*, vol. 245, no. 6, pp. 889–893, 2007.
- [8] M. Frotscher, “Role for Reelin in stabilizing cortical architecture,” *Trends in Neurosciences*, vol. 33, no. 9, pp. 407–414, 2010.
- [9] R. Levi-Montalcini, “The nerve growth factor 35 years later,” *Science*, vol. 237, no. 4819, pp. 1154–1162, 1987.
- [10] M. V. Sofroniew, C. L. Howe, and W. C. Mobley, “Nerve growth factor signaling, neuroprotection, and neural repair,” *Annual Review of Neuroscience*, vol. 24, pp. 1217–1281, 2001.
- [11] G. Carmignoto, L. Maffei, P. Candeo, R. Canella, and C. Comelli, “Effect of NGF on the survival of rat retinal ganglion cells following optic nerve section,” *Journal of Neuroscience*, vol. 9, no. 4, pp. 1263–1272, 1989.
- [12] A. Micera, A. Lambiase, B. Stampachiacchiere, S. Bonini, S. Bonini, and F. Levi-Schaffer, “Nerve growth factor and tissue repair remodeling: trkA^{NGFR} and p75^{NTR}, two receptors one fate,” *Cytokine and Growth Factor Reviews*, vol. 18, no. 3-4, pp. 245–256, 2007.
- [13] M. V. Chao and B. L. Hempstead, “p75 and Trk: a two-receptor system,” *Trends in Neurosciences*, vol. 18, no. 7, pp. 321–326, 1995.
- [14] V. Colafrancesco, M. Coassin, S. Rossi, and L. Aloe, “Effect of eye NGF administration on two animal models of retinal ganglion cells degeneration,” *Annali dell’Istituto Superiore di Sanita*, vol. 47, no. 3, pp. 284–289, 2011.
- [15] Y. Bai, P. Dergham, H. Nedev et al., “Chronic and acute models of retinal neurodegeneration TrkA activity are neuroprotective whereas p75^{NTR} activity is neurotoxic through a paracrine mechanism,” *The Journal of Biological Chemistry*, vol. 285, no. 50, pp. 39392–39400, 2010.
- [16] K. Matsui, S. Furukawa, H. Shibasaki, and T. Kikuchi, “Reduction of nerve growth factor level in the brain of genetically ataxic mice (weaver, reeler),” *FEBS Letters*, vol. 276, no. 1-2, pp. 78–80, 1990.
- [17] A. M. Betancourt, S. C. Burgess, and R. L. Carr, “Effect of developmental exposure to chlorpyrifos on the expression of neurotrophin growth factors and cell-specific markers in neonatal rat brain,” *Toxicological Sciences*, vol. 92, no. 2, pp. 500–506, 2006.
- [18] L. Silver, *Mouse Genetics Concepts and Application*, Oxford University Press, New York, NY, USA, 1995.
- [19] M. Tomomura, D. S. Rice, J. I. Morgan, and M. Yuzaki, “Purification of Purkinje cells by fluorescence-activated cell sorting from transgenic mice that express green fluorescent protein,” *European Journal of Neuroscience*, vol. 14, no. 1, pp. 57–63, 2001.
- [20] J. Oberdick, R. J. Smeyne, J. R. Mann, S. Zackson, and J. I. Morgan, “A promoter that drives transgene expression in cerebellar Purkinje and retinal bipolar neurons,” *Science*, vol. 248, no. 4952, pp. 223–226, 1990.
- [21] G. D’Arcangelo, G. G. Miao, and T. Curran, “Detection of the reelin breakpoint in reeler mice,” *Molecular Brain Research*, vol. 39, no. 1-2, pp. 234–236, 1996.
- [22] M. Coassin, A. Lambiase, V. Sposato, A. Micera, S. Bonini, and L. Aloe, “Retinal p75 and bax overexpression is associated with

- retinal ganglion cells apoptosis in a rat model of glaucoma," *Graefes Archive for Clinical and Experimental Ophthalmology*, vol. 246, no. 12, pp. 1743–1749, 2008.
- [23] A. Micera, I. Puxeddu, A. Lambiase et al., "The pro-fibrogenic effect of nerve growth factor on conjunctival fibroblasts is mediated by transforming growth factor- β ," *Clinical and Experimental Allergy*, vol. 35, no. 5, pp. 650–656, 2005.
- [24] M. W. Pfaffl, "A new mathematical model for relative quantification in real-time RT-PCR," *Nucleic Acids Research*, vol. 29, no. 9, article e45, 2001.
- [25] R. R. Wilcox, "Understanding the practical advantages of modern ANOVA methods," *Journal of Clinical Child and Adolescent Psychology*, vol. 31, no. 3, pp. 399–412, 2002.
- [26] X. Sun, X. Xu, F. Wang et al., "Effects of nerve growth factor for retinal cell survival in experimental retinal detachment," *Current Eye Research*, vol. 32, no. 9, pp. 765–772, 2007.
- [27] A. Lambiase, M. Centofanti, A. Micera et al., "Nerve growth factor (NGF) reduces and NGF antibody exacerbates retinal damage induced in rabbit by experimental ocular hypertension," *Graefes Archive for Clinical and Experimental Ophthalmology*, vol. 235, no. 12, pp. 780–785, 1997.
- [28] C. Harada, T. Harada, K. Nakamura, Y. Sakai, K. Tanaka, and L. F. Parada, "Effect of p75^{NTR} on the regulation of naturally occurring cell death and retinal ganglion cell number in the mouse eye," *Developmental Biology*, vol. 290, no. 1, pp. 57–65, 2006.
- [29] Y. S. Kim, D. H. Jo, H. Lee, J. H. Kim, K. W. Kim, and J. H. Kim, "Nerve growth factor-mediated vascular endothelial growth factor expression of astrocyte in retinal vascular development," *Biochemical and Biophysical Research Communications*, vol. 431, no. 4, pp. 740–745, 2013.
- [30] F. Lebrun-Julien, B. Morquette, A. Douillette, H. U. Saragovi, and A. Di Polo, "Inhibition of p75^{NTR} in glia potentiates TrkA-mediated survival of injured retinal ganglion cells," *Molecular and Cellular Neuroscience*, vol. 40, no. 4, pp. 410–420, 2009.
- [31] R. A. de Melo Reis, M. E. C. Cabral-da-Silva, F. G. de Mello, and J. S. H. Taylor, "Müller glia factors induce survival and neurogenesis of peripheral and central neurons," *Brain Research*, vol. 1205, pp. 1–11, 2008.
- [32] M. Karlsson, R. Mayordomo, L. F. Reichardt, S. Catsicas, H. J. Karten, and F. Hallböök, "Nerve growth factor is expressed by postmitotic avian retinal horizontal cells and supports their survival during development in an autocrine mode of action," *Development*, vol. 128, no. 4, pp. 471–479, 2001.
- [33] M. Rydén, B. Hempstead, and C. F. Ibáñez, "Differential modulation of neuron survival during development by nerve growth factor binding to the p75 neurotrophin receptor," *The Journal of Biological Chemistry*, vol. 272, no. 26, pp. 16322–16328, 1997.
- [34] S. O. Yoon, P. Casaccia-Bonnel, B. Carter, and M. V. Chao, "Competitive signaling between TrkA and p75 nerve growth factor receptors determines cell survival," *Journal of Neuroscience*, vol. 18, no. 9, pp. 3273–3281, 1998.
- [35] P. A. Barker and E. M. Shooter, "Disruption of NGF binding to the low affinity neurotrophin receptor p75(LNTR) reduces NGF binding to TrkA on PC12 cells," *Neuron*, vol. 13, no. 1, pp. 203–215, 1994.
- [36] D. Esposito, P. Patel, R. M. Stephens et al., "The cytoplasmic and transmembrane domains of the p75 and Trk A receptors regulate high affinity binding to nerve growth factor," *The Journal of Biological Chemistry*, vol. 276, no. 35, pp. 32687–32695, 2001.
- [37] G. L. Barrett and P. F. Bartlett, "The p75 nerve growth factor receptor mediates survival or death depending on the stage of sensory neuron development," *Proceedings of the National Academy of Sciences of the United States of America*, vol. 91, no. 14, pp. 6501–6505, 1994.
- [38] K. Lee, K. Bachman, S. Landis, and R. Jaenisch, "Dependence on p75 for innervation of some sympathetic targets," *Science*, vol. 263, no. 5152, pp. 1447–1449, 1994.
- [39] C. A. Bentley and K. F. Lee, "p75 is important for axon growth and Schwann cell migration during development," *Journal of Neuroscience*, vol. 20, no. 20, pp. 7706–7715, 2000.
- [40] R. T. Dobrowsky and B. D. Carter, "p75 neurotrophin receptor signaling: mechanisms for neurotrophic modulation of cell stress?" *Journal of Neuroscience Research*, vol. 61, no. 3, pp. 237–243, 2000.
- [41] T. Yamashita, K. L. Tucker, and Y. A. Barde, "Neurotrophin binding to the p75 receptor modulates Rho activity and axonal outgrowth," *Neuron*, vol. 24, no. 3, pp. 585–593, 1999.
- [42] M. F. DeFreitas, P. S. McQuillen, and C. J. Shatz, "A novel p75^{NTR} signaling pathway promotes survival, not death, of immunopurified neocortical subplate neurons," *Journal of Neuroscience*, vol. 21, no. 14, pp. 5121–5129, 2001.
- [43] B. Hu, H. K. Yip, and K. F. So, "Expression of p75 neurotrophin receptor in the injured and regenerating rat retina," *NeuroReport*, vol. 10, no. 6, pp. 1293–1297, 1999.
- [44] A. Bosco and R. Linden, "BDNF and NT-4 differentially modulate neurite outgrowth in developing retinal ganglion cells," *Journal of Neuroscience Research*, vol. 57, no. 6, pp. 759–769, 1999.
- [45] R. S. Alroy, S. X. Bamji, C. D. Pozniak et al., "P53 is essential for developmental neuron death as regulated by the TrkA and p75 neurotrophin receptors," *Journal of Cell Biology*, vol. 143, no. 6, pp. 1691–1703, 1998.
- [46] A. Cohen, G. M. Bray, and A. J. Aguayo, "Neurotrophin-4/5 (NT-4/5) increases adult rat retinal ganglion cell survival and neurite outgrowth in vitro," *Journal of Neurobiology*, vol. 25, no. 8, pp. 953–959, 1994.
- [47] Y. J. Chang, C. M. Hsu, C. H. Lin, M. S. Lu, and L. Chen, "Electrical stimulation promotes nerve growth factor-induced neurite outgrowth and signaling," *Biochimica Et Biophysica Acta*, vol. 1830, no. 8, pp. 4130–4136, 2013.
- [48] C. Radtke, H. O. Rennekampff, K. Reimers, P. M. Vogt, and J. D. Kocsis, "Paracrine loop of keratinocyte proliferation and directed neuritic outgrowth in a neuroepithelial coculture," *Annals of Plastic Surgery*, vol. 70, no. 2, pp. 162–167, 2013.
- [49] B. D. Carter and G. R. Lewint, "Neurotrophins live or let die: does p75(NTR) decide?" *Neuron*, vol. 18, no. 2, pp. 187–190, 1997.
- [50] A. Micera, I. Puxeddu, B. O. Balzamino, S. Bonini, and F. Levi-Schaffer, "Chronic nerve growth factor exposure increases apoptosis in a model of in vitro induced conjunctival myofibroblasts," *PLoS ONE*, vol. 7, no. 10, Article ID e47316, 2012.
- [51] E. M. Wexler, O. Berkovich, and S. Nawy, "Role of the low-affinity NGF receptor (p75) in survival of retinal bipolar cells," *Visual Neuroscience*, vol. 15, no. 2, pp. 211–218, 1998.
- [52] C. L. Cepko, C. P. Austin, X. Yang, M. Alexiades, and D. Ezzeddine, "Cell fate determination in the vertebrate retina," *Proceedings of the National Academy of Sciences of the United States of America*, vol. 93, no. 2, pp. 589–595, 1996.
- [53] Q. Yan, J. Wang, C. R. Matheson, and J. L. Urich, "Glial cell line-derived neurotrophic factor (GDNF) promotes the survival of axotomized retinal ganglion cells in adult rats: comparison

to and combination with brain-derived neurotrophic factor (BDNF),” *Journal of Neurobiology*, vol. 38, no. 3, pp. 382–390, 1999.

- [54] F. Lebrun-Julien, M. J. Bertrand, O. de Backer et al., “ProNGF induces $\text{TNF}\alpha$ -dependent death of retinal ganglion cells through a p75^{NTR} non-cell-autonomous signaling pathway,” *Proceedings of the National Academy of Sciences of the United States of America*, vol. 107, no. 8, pp. 3817–3822, 2010.



Hindawi

Submit your manuscripts at
<http://www.hindawi.com>

